Adsorption of homopolypeptides on gold investigated using atomistic molecular dynamics

Ana Vila Verde[1], *Peter J. Beltramo*[2], *Janna K. Maranas*[3*]

[1] University of Minho, Department of Physics, Braga, Portugal and FOM Institute AMOLF, Amsterdam, The Netherlands

[2] University of Delaware, Department of Chemical Engineering and Center for Molecular and Engineering Thermodynamics, USA

[3] The Pennsylvania State University, Department of Chemical Engineering, USA

AUTHOR EMAIL ADDRESS: jmaranas@psu.edu

CORRESPONDING AUTHOR FOOTNOTE: *Janna K. Maranas, 155 Fenske Laboratory, University Park, PA 16802, USA. E-mail: jmaranas@psu.edu. Phone:+1 (814) 863-6228. Fax:+1 (814) 865-7846.

ABSTRACT

We investigate the role of dynamics on adsorption of peptides to gold surfaces using all-atom molecular dynamics simulations in explicit solvent. We choose six homopolypeptides [Ala_{10}, Ser_{10}, Thr_{10}, Arg_{10}, Lys_{10}, and Gln_{10}], for which experimental surface coverages are not correlated with amino acid level affinities for gold, with the idea that dynamic properties may also play a role. To assess dynamics we determine both conformational movement and flexibility of the peptide within a given conformation. Low conformational movement indicates stability of a given conformation and leads to less adsorption than homopolypeptides with faster conformational movement. Likewise, low flexibility within a given conformation also leads to less adsorption. Neither amino acid affinities nor dynamic considerations alone predict surface coverage; rather both quantities must be considered in peptide adsorption to gold surfaces.

KEYWORDS: Peptide adsorption; gold binding peptides; homopolypeptides; all-atom molecular dynamics simulations; peptide flexibility; peptide stability

Introduction

Interactions between proteins and inorganic surfaces occur frequently in natural systems. For example, the formation of dental enamel, bone, mother-of-pearl or the silica shell of marine microorganisms requires the presence of specific proteins. These proteins drive precipitation of the inorganic fraction from solution to form nanoparticles and/or direct the self-organization of those nanoparticles forming materials with well-defined nanostructures.[1-3]

Proteins involved in the formation of natural nanostructured materials often adsorb strongly to the inorganic material involved, and less strongly to other materials. Recognition of these two characteristics inspired researchers to use high-throughput combinatorial techniques to isolate artificial proteins and peptides showing high affinity for particular inorganic materials, i.e. showing both strong and specific adsorption to a material. In this context, "strong" means that the free energy of adsorption is less than -40 kJ/mol and "specific" means that the protein adsorbs strongly to a particular surface but not others. Examples of surfaces for which artificial peptides with high affinity have been identified include Au,[4,5] Ag,[6] ZnO,[7,8] GaAs,[9] SiO_2,[3,10,11] or CuO_2.[8]

Examination of the composition of peptides with high affinity for various surfaces shows that the 20 natural amino acids are not equally represented. This is expected, as the side chain chemistry differs greatly between amino acids. This observation leads to a closer examination of the issue of the intrinsic affinity of amino acids for various surfaces using both experiments and simulations. In one set of experiments, aqueous solutions containing homopolypeptides 10 amino acids long were put in contact with various inorganic surfaces, and the peptide surface density (σ_{ads}) was measured.[12] The authors found that homopolypeptides have varying affinities for the same surface. For insulator or oxide surfaces, which are charged, the observed trends are clear: homopolypeptides with opposite charge have the highest affinity for the surface. In contrast, no clear trends were observed for metals.

For example, the homopolypeptides Ser_{10}[13] (decaserine, polar), Arg_{10} (decaarginine, polar, charged), Thr_{10} (decathreonine, polar) and Iso_{10} (decaisoleucine, apolar) adsorb on gold with similar affinity, but other homopolypeptides with equivalent polarity and charge have substantially lower affinity for that metal. The interaction between single amino acids and gold was also examined with classical all-atom simulations using a polarizable model for gold and explicit solvent.[14-16] The adsorption free energy (ΔG_{ads}) of each amino acid obtained in those simulations argues that different amino acids have widely varying affinities for gold, but the trends observed in simulation differ from those found in the homopolypeptide experiments. For example, the simulations indicate that the tyrosine amino acid has the highest affinity for gold (ΔG_{ads} = - 44.2 kJ/mol) so the 0^{th} order estimate of the adsorption free energy of Tyr_{10} is -442 kJ/mol. Instead, experiments show that Tyr_{10} does not adsorb to any appreciable extent as a homopolypeptide.

The observed discrepancy in surface affinity between experiments with homopolypeptides and simulations with amino acids can have several origins. It could arise from deficiencies in the force-field used in the simulations or because the amino acid termini dominate the interactions with the surface for single amino acids. Since the influence of the peptide termini is felt less intensely in the case of homopolypeptides, adsorption affinities of homopolypeptides do not necessarily map directly to amino acid affinities for the same surface. Previous work suggests that a third possibility may also control the different affinities of homopolypeptides and individual amino acids for surfaces. Simulations using generic peptide models and surfaces suggest that peptide structure, structural stability and flexibility (characteristics dictated by the identity and sequence of amino acids in a peptide) are critical for adsorption.[17,18] Our previous work confirmed that this is the case for adsorption of three different peptides on gold.[19] We used classical all-atom simulations in explicit water with a non-polarizable force field to investigate adsorption of three genetically engineered peptides [total length 84 amino

acids] with varying affinity for gold: two gold binding peptides and one non gold binding peptide. Despite having different affinities for gold, all three peptides have the same fraction of amino acids with high affinity for gold as homopolypeptides. Our results suggested that adsorption differences arose from differences in peptide structure, structural stability and flexibility. Stability reflects the extent to which peptides maintain their structure, whereas flexibility reflects the broadness and frequency of oscillations around the stable peptide conformation. Results indicated that low peptide stability and high flexibility enable the formation of multiple peptide-gold contacts and thus high peptide affinity for this metal.

This work examines the issue of homopolypeptide dynamics in adsorption to gold using atomistic molecular dynamics simulations. We choose gold because understanding peptide adsorption to this metal is particularly important: its biocompatibility makes it a promising material for bioelectronics and nanomedicine.[20,21] We select six homopolypeptides for our study: Ser_{10}, Arg_{10}, Thr_{10}, Lys_{10}, Ala_{10} and Gln_{10}. As summarized in Table 1, experiments show that the first three remain adsorbed on gold surfaces even after the surface is washed whereas the last three do not.[12] Both the gold-adsorbing Arg_{10} and the non gold-adsorbing Lys_{10} have a charge of $+10e$, where e is the absolute value of the electron charge; the remaining peptides are neutral. These particular peptides were selected out of the 20 experimentally tested by Willet et al.[12] to ensure that both adsorbing and non adsorbing peptides comprised neutral and charged peptides, helical/non-helical structures, and their constituting amino acids had different affinities for the surface, as shown in table 1.

Table 1. Properties of the simulated homopolypeptides and the corresponding individual amino acids. The experimentally determined affinity of each homopolypeptide for gold is given as the adsorbed surface density σ_{ads}.[12] Homopolypeptides with adsorbed surface densities lower than $0.5*10^3/\mu m^2$ are considered non-adsorbed. The affinity of individual amino acids for gold is given as the adsorption free energy (ΔG_{ads}) determined from simulation.[15] The initial configuration used for the simulations in solution and the final configuration at the end of those simulations are also shown (RC/E=random coil/extended configuration).

Peptide	Charge, *e*	Initial configuration	Final configuration	Peptide σ_{ads}, $10^3/\mu m^2$	Amino acid ΔG_{ads}, kJ/mol
Lys_{10}	+10	sheet	RC/E	<0.5	-30.0
Ala_{10}	0	helix	RC/E	<0.5	-21.9
Gln_{10}	0	helix	helix	<0.5	-28.6
Ser_{10}	0	helix	RC/E	0.9	-23.1
Arg_{10}	+10	sheet	RC/E	1.2	-36.3
Thr_{10}	0	sheet	RC/E	1.6	-28.9

We investigate the last stages of adsorption, during which individual peptides approach the gold surface from solution and come in direct contact with that surface. Experiments indicate that the fraction of the surface area covered by the peptide is small, of order 0.1%.[12] In this regime we do not expect surface cluster formation and growth to occur, even though it has been suggested that these two mechanisms play a role in adsorption of gold binding peptides that achieve higher surface coverages.[22,23] To understand how adsorption affects peptide conformation and conformational stability/flexibility, we also examine the behavior of free peptides in solution. We conclude by connecting the peptide affinities for gold and peptide dynamics observed in our simulations with experimentally observed homopolypeptide affinities for gold and reported amino acid affinities for this metal obtained from simulations.

Experimental section

We use methodology similar to our prior study of 84 amino acid gold binding and non-gold binding peptides.[19] We use molecular dynamics simulations with explicit solvent to investigate the behavior of the homopolypeptides in question in solution and on gold at a neutral pH of 7. The CHARMM22 force-field is used for the peptides and buffering ions and the modified TIP3P (mTIP3P) model is used for water.[24,25] The gold surface is modeled at the classical level using the Lennard-Jones potential previously derived by us.[19] The surface structure in experimental studies was not characterized, and thus we choose the (001) surface because it is computationally convenient. We do not advance the positions of gold atoms in time and allow neither chemisorption nor gold polarization. While the assumptions underlying modeling of the gold surface necessarily limit the results, there is evidence that all are reasonable for the nature of our investigation. Significant movement of atoms in a metal surface in a time scale < 200 ns is not expected. Chemisorption is significant only for cysteine,[26,27] an amino acid we do not consider. Studies of water on metal surfaces with and without polarization indicate that the interaction of charges with their images largely results in cancellation, and the energy from polarization is less than 10% of the total energy. This is consistent with observations indicating that the surface structure of water on metals is mostly unaffected by the inclusion of metal polarizability.[28,31] The limited duration of all-atom molecular dynamics simulations makes the study of the entire process of adsorption – which includes movement of peptides within hundreds of nanometers from the gold surface and multiple adsorptions and desorptions – computationally unfeasible. One can either follow multiple adsorptions from various initial configurations for a short time [10-15 ns] or follow a single event until the fraction of adsorbed amino acids remains constant [for these peptides 75-170 ns]. The former is preferable for assessing free energies of adsorption[18] and the latter for generating long trajectories from which dynamic properties following adsorption may be accurately determined. We generate one long adsorption trajectory for each homopolypeptide.

Simulations are performed using the simulation package NAMD - Scalable Molecular Dynamics.[32] The package VMD - Visual Molecular Dynamics is used to visualize and analyze trajectories.[33] Equilibration of all systems is done using the NPT ensemble at one atmosphere and 310 K. The pressure is controlled through a modified Nosé-Hoover barostat with Langevin dynamics to control fluctuations. The temperature is maintained using Langevin dynamics, except for equilibration of systems with gold surfaces where we use an Andersen thermostat because combining the barostat, fixed X and Y dimensions, and the Langevin thermostat introduces computational instability. For production runs we use the NPT ensemble for systems without a gold surface. For systems with a gold surface, we switch to the NVT ensemble so that Langevin dynamics may be used to control temperature. Van der Waals interactions are modified at distances beyond 10 Å so they smoothly become zero at 12 Å. Electrostatic interactions are calculated directly up to distances of 12 Å; for larger separations we use the Particle Mesh Ewald method with a grid spacing of 1 Å. Integration uses a modified Verlet algorithm with 1 fs time-steps. Bonded forces are calculated at every time-step and van der Waals forces and electrostatics at every two and four steps, respectively. Parallelepiped simulation boxes with periodic boundary conditions are used in all simulations. The box size is selected so that the protein and its nearest periodic images are separated by at least 12 Å to ensure that the periodic images of the protein do not interact via van der Waals potentials.

We require the solution structure of the homopolypeptides to generate the starting configurations for MD simulations. These structures are not available in the Protein Data Bank and cannot be predicted using available structure prediction packages like Robetta because these packages should only be used to predict the structure of longer peptides.[34] We estimate the peptide's solution structure based on available experimental information on peptides of similar length and composition, and MD simulations in water. Available reports indicate that short peptides predominantly composed of glutamine, alanine or serine have some helical structure in solution, whereas short threonine, arginine or lysine peptides do

not.[35-40] As these studies focused on peptides similar, but not identical, to those used here, we took the following approach to determine appropriate initial structures for our simulations: peptides with little reported tendency to form helices were simply initiated in an extended sheet structure. Peptides with some propensity to form alpha-helices in solution were initialized in that conformation. If an alpha-helix is not in fact the stable conformation of a peptide at the temperature, pressure and salt concentration used in our simulations, we expect that it will quickly melt during the simulation; if the helix does not melt then this indicates it is at least a local energy minimum configuration of the peptide, and as such a relevant conformation to be investigated. We use the molecular builder Molden to generate the alpha-helical or extended sheet initial structures.[41] Each structure is surrounded with 20 Å of 0.1 M KCl aqueous solution using the equilibrated water box feature in VMD. Each solvated peptide is then simulated for 30 ns at 310 K to evaluate its conformational stability as described in the Results section. The most representative structure for each peptide at the end of these simulations is selected as starting point for simulations with Au(001) surfaces. Each peptide is placed at the XY center of the surface, with the peptide atoms at least 20 Å from the gold, and surrounded with 20 Å of water and 0.1 M KCL from all sides. This thickness of water ensures that bulk water behavior is recovered between the peptide and the gold surface.[19,42] Because the LJ potential is short ranged, the gold surface is limited to four atomic layers. The simulation cell sizes and the total number of atoms are presented in Tables 1 and 2 of the Supporting Information. Details of the minimization and equilibration procedure can also be found there. Production runs for proteins in solution are 30 ns. Adsorption simulations are run for a minimum of 75 ns, or until the fraction of adsorbed atoms remains stable for 20 ns.

Results and discussion

Starting homopolypeptide structures. As described above, the stability of each initial structure was tested by simulating it for 30 ns at 310 K. To quantify the magnitude of structural changes experienced by each peptide we monitor both the percent change in the radius of gyration R_g and local changes in backbone conformation throughout the entire simulation. R_g reflects changes in the overall size of the peptide, so differences in R_g reveal changes in conformation. Local peptide backbone conformations are well-characterized by the dihedral angles formed by four consecutive α-carbons because these dihedrals take well-defined values for particular backbone conformations (e.g. helices or sheets).[43] To monitor changes in backbone conformation we calculate the probability distribution function of each dihedral angle over the entire simulation.

As illustrated in Figure 1, Gln_{10}, initially a helix, changes conformation the least of all six peptides. R_g changes by only 3% and the dihedral probability distribution function is narrowly distributed around the initial value [indicated by an arrow in the Figure]. Visual inspection of the trajectory confirms that Gln_{10} maintains its original helical conformation at the end of the 30 ns simulation. Because Gln_{10} does not change configuration, we can use its dihedral distribution to define a criterion for lack of backbone conformational changes: a distribution of dihedrals with width smaller than two standard deviations for Gln_{10}, or 40º. Dihedral distributions wider than this indicate conformational change. Ala_{10}, initially also a helix, behaves opposite to Gln_{10}: the distribution of α-carbon dihedrals is wide with little indication of peaks, and the average variation in R_g is 24%, the largest among all homopolypeptides. Inspection of the trajectory confirms that Ala_{10}'s helical conformation rapidly disappears and it assumes extended, flexible conformations. Significant conformational change was also observed in analogous simulations of Ala_{10} using the Consistent Valence Force Field [CVFF], suggesting this behavior is robust.[44] The remaining peptides - Thr_{10}, Ser_{10}, Arg_{10} and Lys_{10} - show intermediate

behavior: changes in R_g fall between 7 and 20%, and dihedral distributions indicate changes in conformation according to the criteria above [width of distribution is larger than 40º] and visual inspection. The two indicators of conformational change do not always correspond. For example, variations in R_g for Lys_{10} [7%] and Thr_{10} [20%] suggest these two peptides behave differently, while their dihedral distributions are similar. This occurs due to conformational change that does not result in size variations, and means the distribution of backbone dihedrals is a more reliable indicator of conformational change.

Because our adsorption simulations follow a single trajectory for each homopolypeptide, it is important to wisely select the initial conformation used in adsorption simulations. This conformation is selected based on the solution simulations. Gln_{10} maintains a clearly defined and stable helical conformation in solution, which we use as the starting point for the adsorption simulation of this peptide. In contrast, the data for the other peptides shown in Figure 1 indicate that they do not have a stable conformation in solution. Instead, they assume a broad ensemble of conformations that can collectively be described as extended random coils. Since no preferred conformation exists for the conformationally labile peptides, we take the last conformation at the end of the simulations in solution as the initial structure for the adsorption simulations. The initial and final configurations from the simulations of homopolypeptides in solution are summarized in Table 1.

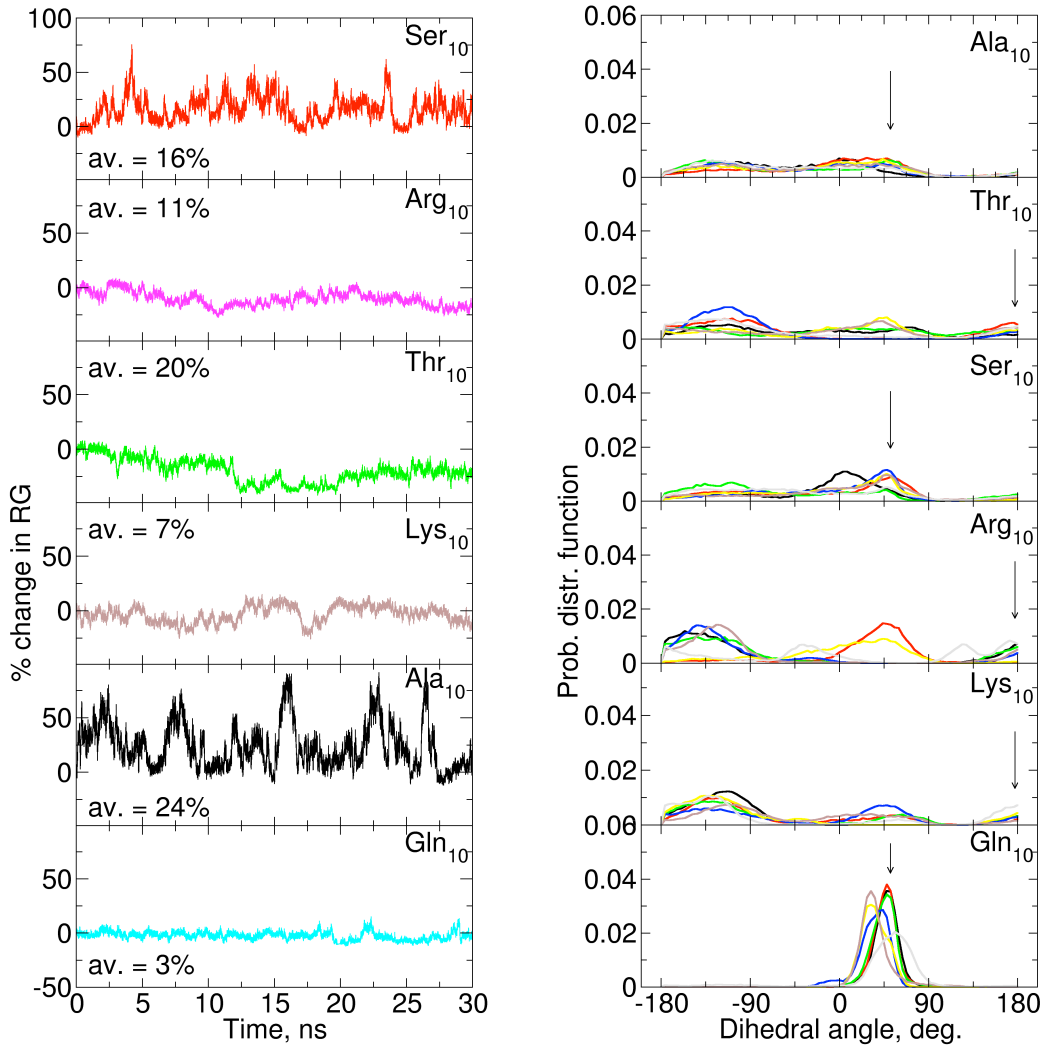

(a) (b)

Figure 1. Conformational changes of homopolypeptides in solution. (a) Percent change in the radius of gyration. The average of the absolute value of % percent change in R_g is indicated in each graph. (b) Probability distribution functions of each dihedral angle formed by four consecutive α-carbons. Each color refers to one dihedral. The arrows indicate the initial value of the dihedrals for each peptide.

Simulations of peptides on gold. As mentioned above, the simulations with gold surfaces were run for a minimum of 75 ns and were terminated once the fraction of adsorbed atoms at the surface remained approximately constant for at least 20 ns. We consider an atom adsorbed if it displaced the first water layer from the surface. Support for this criterion comes from existing computational studies of adsorption of biomolecules on metals using either computational approaches similar to that used here[45] or ab initio molecular dynamics.[26] As the first and second peaks of the water density perpendicular to the surface show a minimum at ~5 Å,[19] an atom is adsorbed if it is within 5 Å of the plane defined by the centers of mass of the top gold atoms.

Figure 2 shows the percentage of atoms of each homopolypeptide that are adsorbed as a function of time. All peptide atoms are initially at least 20 Å from the gold surface, as described in the Methods section. Ser_{10} and Ala_{10} initiate contact with the gold surface in less than 2 ns, and a large fraction [> 50%] of their atoms adsorb. Qualitatively similar behavior has also been observed for Ala_{10} using the CVFF force field.[44] Arg_{10}, Thr_{10} and Gln_{10} initiate contact after 12 to 30 ns. The initial fractions of adsorbed atoms [50%] are similar for Arg_{10} and Thr_{10}, and Arg_{10} has a second adsorption step at 50 ns. Gln_{10} has 30% of its atoms adsorbed. Lys_{10} does not adsorb until 75 ns and the fraction adsorbed is similar to Gln_{10}. Differences in the time to initial contact reflect the different distances between the peptides and the gold surfaces that arise after minimization and equilibration. At the end of the simulation all peptides are in direct contact with the surface, indicating that all have some affinity for gold.

These simulations give insight into a single adsorption event for each peptide, but do not ensure that system configurations are sampled in proportion to their equilibrium probability. It is important to discuss how this limitation affects comparison between reported experiments and the results shown in Figure 2. Ideally, one would observe many adsorption and desorption events, and from their relative probability calculate the free energy of adsorption for each peptide. Since accurate calculation of

dynamic properties requires long simulation runs, and multiple simulations of the required duration are computationally infeasible, we must find a way to estimate the extent of adsorption from a single adsorption event. Here we consider if using the percentage of adsorbed atoms from a single adsorption event can serve as an indicator of peptide affinity for a surface. We compare this measure of the affinity of each homopolypeptide for gold with experimentally determined surface coverages[12] in Figure 3. Remarkably, the two follow the same trends, although quantitative agreement is lacking. Similar trends have also been observed in classical simulations of adsorption of peptides of similar[44] and longer length[19] on metals. If we divide the peptides into good adsorbers (Thr_{10}, Arg_{10}, Ser_{10} and Ala_{10}, with 50% or more atoms on the surface) and poor adsorbers (Gln_{10} and Lys_{10}, with less than 40% atoms on the surface), the two groups coincide. The exception is alanine: while experiments have shown that Ala_{10} adsorbs poorly on gold, in our simulations 70% of its atoms are on the surface. Alanine-rich peptides 15 or 21 amino acids long are known to form fibrils,[46] and thus simulations of a single Ala_{10} homopolypeptide may not be representative.

It is also important to address the appropriateness of the force field. Force field limitations will be largest in the case of polar or charged amino acids because gold polarizability is not included in our simulations. The homopolypeptide that most diverges from experimental data is Ala_{10}, with a non-polar, uncharged side group; the remaining peptides display qualitative agreement with no obvious outliers. Taken together, these results suggest that the force field used is sufficient for our study.

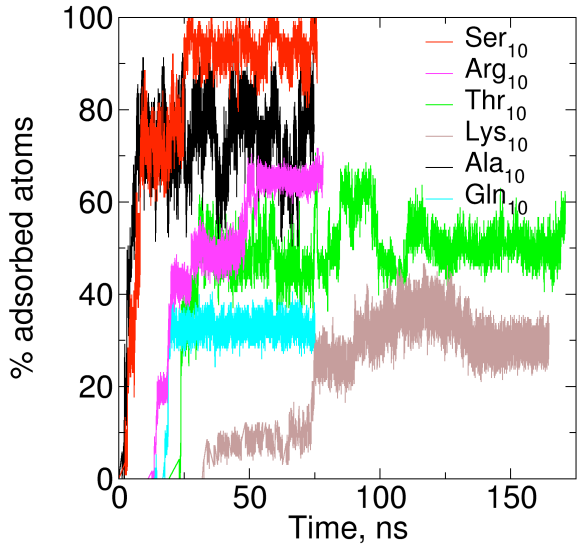

Figure 2. Percentage of atoms adsorbed on gold as a function of time. The first nonzero data point represents the time at which the first atom adsorbs.

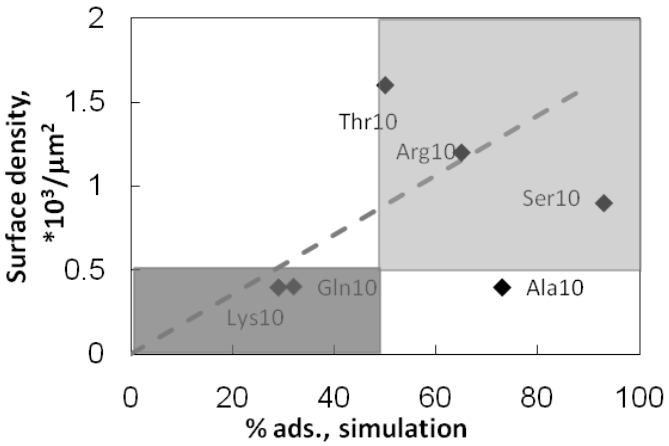

Figure 3. Peptide affinities for gold from experiment and simulation. Y-axis: adhered peptide density σ_{ads} from fluorescence experiments.[12] X-axis: percentage of adsorbed amino acids from simulation. The experimentally determined surface coverage for Lys_{10}, Gln_{10} and Ala_{10} is reported in the original reference as "< 0.5 $*10^3$ /μm^2", and is depicted in this graph as 0.4 $*10^3$ /μm^2. Dark grey shading: regions with low affinity for gold [$\sigma_{ads} < 0.5*10^3/\mu m^2$ (experiment) or less than 50% adsorbed amino acids (simulation)]. Light grey shading: regions with high affinity for gold. Dashed line: perfect linear correlation.

We now ask if adsorption is accompanied by conformational change by examining the radius of gyration and probability distribution of dihedrals. These are the same indicators presented in Figure 1; here we consider them during adsorption to the gold surface, rather than in solution. To facilitate comparison between the radius of gyration of each peptide and the percentage of adsorbed amino acids as adsorption progresses, we juxtapose them in Figure 4a. The dihedral probability distribution functions for all peptides are shown in Figure 4b. The connection between conformational changes and more extensive adsorption than that allowed by the peptide conformation at first contact with the surface is visible for Ser_{10} and Ala_{10}. Between 0 and 20 ns, the percentage of adsorbed atoms in Ala_{10} and Ser_{10} peptides increases by >75% while the radius of gyration varies by >50%. Examination of Figure 4b indicates that the backbone dihedrals do not remain within 40º of their values at t = 0, confirming that conformational changes occur. Gln_{10}, Lys_{10}, Thr_{10} and Arg_{10} undergo initial adsorption without a simultaneous change in radius of gyration. This indicates that either they adsorb as a rigid body, or the conformational changes that occur do not lead to changes in size. For Gln_{10}, the first is true: the percentage of adsorbed atoms increases at t = 20 ns in a quasi step-wise fashion without corresponding changes in the radius of gyration (Figure 4a). This constant size is related to lack of conformational change, as indicated by the dihedral angle distributions, which are tightly clustered around the initial values (Figure 4b). Visual inspection of the trajectory confirms that Gln_{10} approaches and adsorbs on the surface as a helix. The geometry of a helix allows only a certain fraction of the atoms to contact the surface; more extensive adsorption would require conformational changes. Although the peptide sizes of Thr_{10}, Lys_{10} and Arg_{10} change little during initial adsorption, the distribution of their dihedrals suggests that changes in conformation occur even if they do not lead to significant changes in size, as illustrated for Arg_{10} in Figure 1 of the Supporting Information. With the

exception of one dihedral in Thr_{10}, initial values are not maintained. Similarly, all seven dihedrals in Lys_{10} and Arg_{10} and six dihedrals in Thr_{10} change by > 40º, whereas none of the dihedrals in Gln_{10} meet this criterion. In all three peptides, it appears that this conformational freedom leads to changes in adsorption following the initial event. For example, Thr_{10} initially adsorbs on the surface analogously to a rigid body, as indicated by the step-wise change in the fraction of adsorbed atoms at t = 25 ns. Between t = 25 and t = 35 ns, the fraction of adsorbed atoms changes by 20% while the radius of gyration changes by the same value. Arg_{10} has a series of stepwise adsorption events, and Lys_{10} also has small changes in adsorption following the initial event. These contrast with Gln_{10} for which the fraction of adsorbed atoms is constant following initial adsorption. We note that upon adsorption the fluctuations in R_g for Lys_{10} become very small (comparable to those experienced by Gln_{10}). This observation will be discussed during the analysis of peptide flexibility and stability below.

Except for Lys_{10}, conformational flexibility leads, either in the initial event or via conformational changes following initial adsorption, to a higher percentage of atoms adsorbed on the surface (greater than 50%). The reason for this exception is unclear. It is possible that Lys_{10} would adsorb more extensively in longer simulations, although we note that it does not adsorb strongly in the experiments of Willett et al..[12] This suggests that Lys_{10} becomes stiffer upon adsorption and is then unable to further change conformation to achieve more extensive contact with the gold, despite the duration of observation. Similar behavior is noted for Arg_{10} starting at its last adsorption step (60 ns).

From our simulations of free and adsorbed homopolypeptides we conclude that backbone conformational changes favor adsorption. Peptides sampling a variety of conformations in solution also sample more conformations after adsorption, and for this reason adsorb more extensively than those with highly stable conformations in solution. This trend is not quantitative, partially because the affinity of each amino acid for the surface also matters in adsorption.

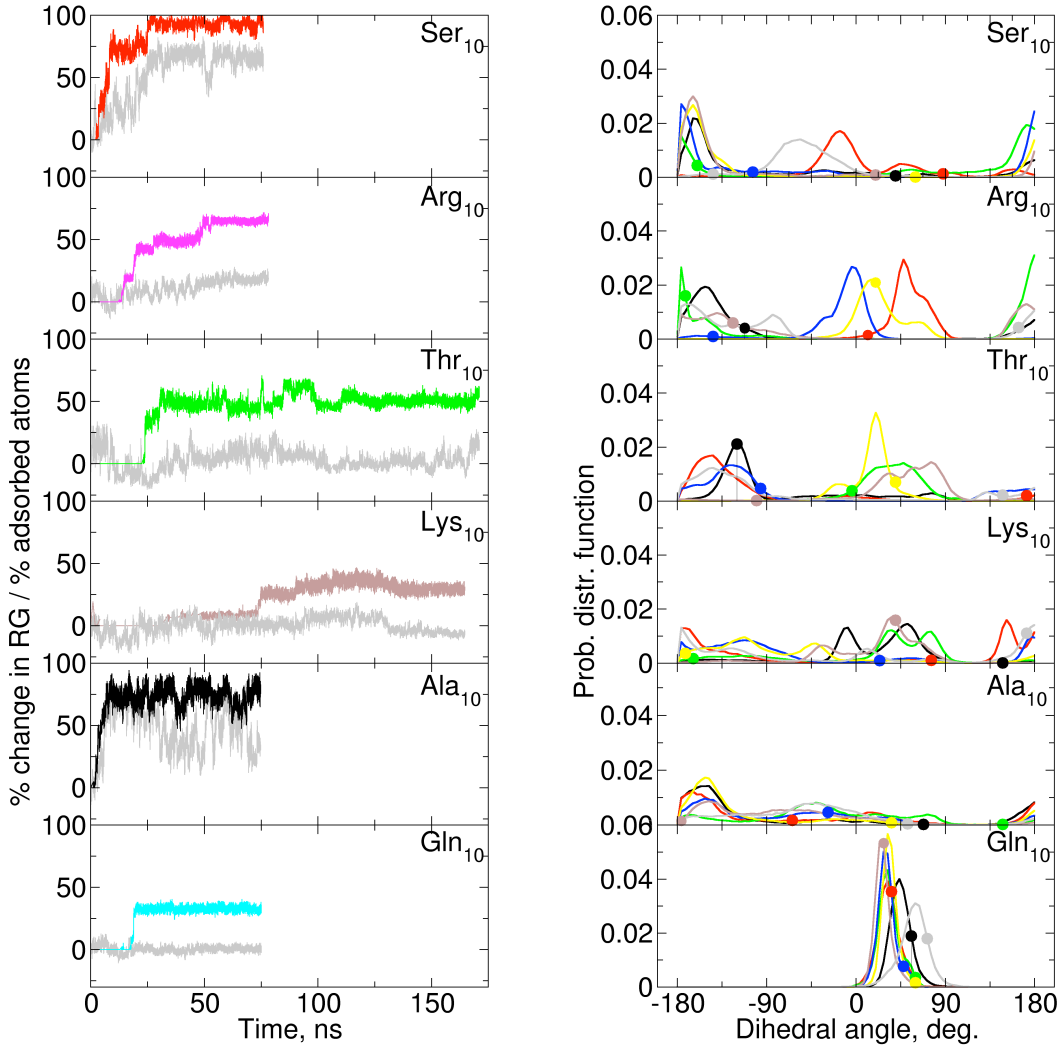

Figure 4. (a) Percent change in the radius of gyration (in gray) and percentage of adsorbed amino acids (other colors) during adsorption simulations. (b) Probability distribution functions of each dihedral angle formed by four consecutive α-carbons during adsorption simulations. Each color refers to a single dihedral. The filled circles indicate the value of each dihedral at the start of the simulation (before adsorption occurs).

Stability and flexibility of free and adsorbed peptides: Having established that peptide conformational changes enable adsorption, we now quantify this influence via peptide stability and flexibility, both before and after adsorption. As mentioned above, peptide backbone stability reflects

the extent to which the peptide remains in a given conformation at longer time scales whereas flexibility refers to oscillations around a stable conformation characteristic of shorter time scales. To quantify stability and flexibility we have monitored changes in α-carbon dihedrals ϕ during a time interval τ using the function

$$C_{dhd}(\tau)=<|\phi_{t+\tau}-\phi_t|> \quad (1)$$

where the average is over all possible time origins *t*. This function varies between 0 and 180°, where 0 corresponds to the limit of no change and 180° the maximum possible change. This function tracks stability when the time interval τ is large, and flexibility if it is small. We have selected τ = 2.5 ns to investigate peptide stability and τ = 0.01 ns for flexibility, for the reasons detailed in our previous publication.[19]

Flexibility is also quantified using a second quantity, the average volume explored by each α-carbon, $V_{\alpha C}$. This quantity has the advantage over C_{dhd}(0.01 ns) of being more intuitive and of giving information on flexibility at the length scale of single amino acids whereas C_{dhd}(0.01 ns) reflects the flexibility over four consecutive amino acids. As in our previous work, $V_{\alpha C}$ is estimated as the product of the X, Y and Z absolute displacements of each α-carbon over 2.5 ns, after removing translation and rotation. This large time interval captures the effect of many fast oscillations of the carbon position around a stable configuration. Atoms that explore larger local volumes are embedded in a more flexible environment than those that do not.

We now compare flexibility and stability of free and adsorbed peptides [Figure 5]. In part (a) of the Figure we consider stability via C_{dhd}(2.5 ns). The smaller values of C_{dhd}(2.5 ns) for the adsorbed peptides confirm that peptide stability increases with adsorption. Analogous changes in peptide stability upon adsorption were also observed when considering peptides 84 amino acids long, as described in our previous work[19] and illustrated in Figure 5.[46] It is interesting to examine the behavior

of Gln_{10}, since it retains its helical structure in solution, and adsorption may denature existing secondary structure. Although Gln_{10} has one of the more favorable ΔGs of adsorption,[15] it retains its helical structure with increased stability. Thus, we conclude that adsorption increases the stability of secondary structure despite its favorable interaction with the surface.

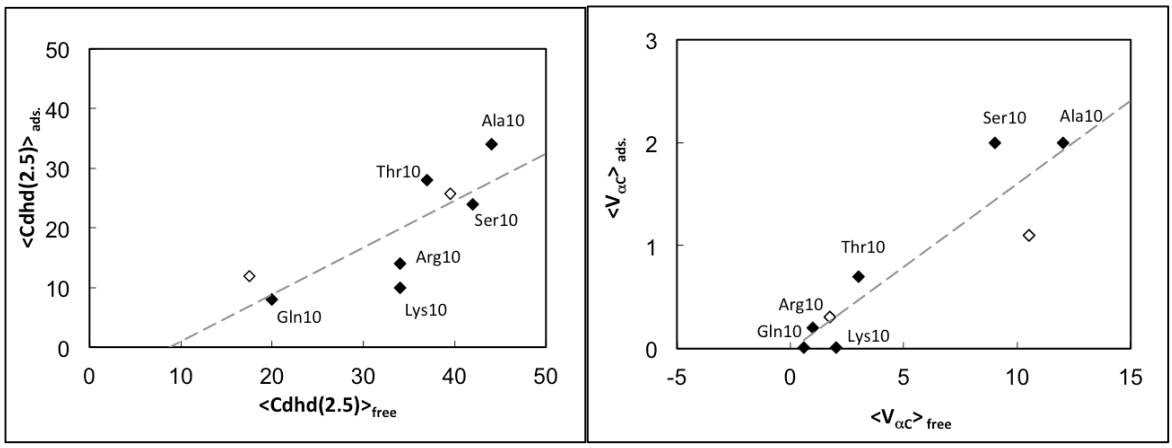

(a) (b)

Figure 5. Correlation between: (a) mean peptide stability of free and adsorbed peptides, as measured by C_{dhd}(2.5 ns); (b) mean peptide flexibility also of free and adsorbed peptides, as measured by $V_{\alpha C}$. Filled symbols: the six homopolypeptides under study here. Empty symbols: previously reported results for two peptides 84 amino acids long.[19] The line is a linear fit to all data points.

Flexibility of the peptide about a particular conformation is expected to lead to more frequent transitions between conformations, i.e. decreased stability. As discussed above, peptide stability increases upon adsorption, so we anticipate flexibility to be simultaneously reduced. Figure 5 confirms that this expected behavior is observed. As with stability, the ordering of flexibilities is unchanged by adsorption to the surface.

In Figure 6, we consider the correlation between dynamic properties and experimentally observed surfaces coverages. From Figure 5, we note that trends among homopolypeptides are similar regardless of the dynamic indicator [$C_{dhd}(2.5\text{ ns})_{ads.}$, $C_{dhd}(2.5\text{ ns})_{free}$, $V_{\alpha C,free}$, $V_{\alpha C,ads.}$]. Here we choose

$C_{dhd}(2.5\ ns)_{ads}$ because adsorption of two of the homopolypeptides [Arg_{10} and Lys_{10}] is limited by reduced conformational exploration after binding. With the exception of Ala_{10}, there is a reasonable correlation between peptide dynamics and surface coverage.

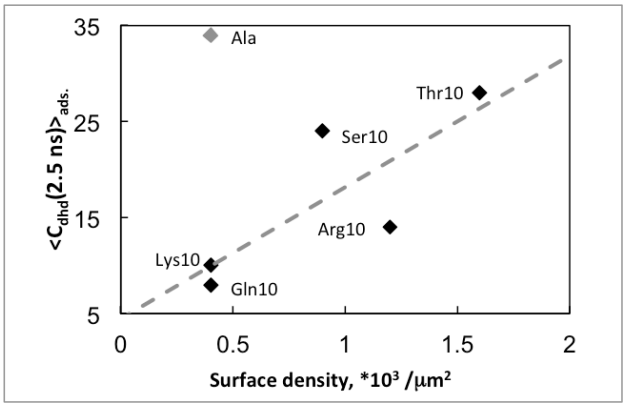

Figure 6. Correlation between experimentally determined peptide affinity for gold (adsorbed surface density) and conformational stability of the adsorbed peptides ($C_{dhd}(2.5\ ns)$). The line is a fit to all points except Ala_{10}.

We summarize our results in schematic form in Figure 7. Also included are the homopolypeptide [experimental surface coverages][12] and the amino acid level ΔG_{ads} [from classical simulations using a polarizable model of gold][15] for gold in aqueous solution. It is clear from this Figure that neither amino acid affinities, nor stability/flexibility alone can explain the experimental results. Instead, binding of a peptide to a gold surface requires both amino acid level affinity *and* low stability of the peptide as a whole. To explore this idea, we consider the product of the absolute value of ΔG_{ads} and the numerical indicator of conformational change, $C_{dhd}(2.5\ ns)_{ads}$. Ultimately binding requires conformational change both in solution [i.e. as the initial contact is made] and during the adsorption event. Here we choose the adsorbed conformational indicator because two of the peptides that adsorb extensively in experimental studies [Arg_{10} and Thr_{10}] adsorb in several steps in our

simulations. The last row in Figure 7 displays the product $\Delta G_{ads} \times C_{dhd}(2.5\ ns)_{ads}$. It is clear that this product more closely follows the experimental observations than either quantity alone. The peptides that bind extensively as homopolypeptides are Arg_{10}, Ser_{10}, and Thr_{10}. Arginine has a very high amino acid affinity for gold ($\Delta G_{ads,Arg}$ = -36.3 kJ/mol), which overcomes its limited flexibility and propensity for conformational change ($<C_{dhd}(2.5\ ns)>_{Arg10,\ ads.}$ = 14º, $V_{\alpha C,\ Arg10,\ ads}$ = 0.2 Å^3). The resulting homopolypeptide binding ($\sigma_{ads,Arg10}$ = 1.2*10^3 /μm^2) is intermediate. Serine has a similar level of homopolypeptide binding ($\sigma_{ads,Ser10}$ = 0.9*10^3 /μm^2), but it results from the opposite combination. The amino acid affinity of serine for gold is low ($\Delta G_{ads,Ser}$ = -23.1 kJ/mol), but dynamic characteristics are favorable ($<C_{dhd}(2.5\ ns)>_{Ser10,\ ads.}$ = 24º, $V_{\alpha C,Ser10,\ ads}$ = 2 Å^3). Threonine has the highest level of binding as a homopolypeptide ($\sigma_{ads,Thr10}$ = 1.6*10^3 /μm^2); a result of intermediate amino acid affinity ($\Delta G_{ads,Thr}$ = -28.9 kJ/mol) and propensity for conformational change ($<C_{dhd}(2.5\ ns)>_{Thr10,\ ads.}$ = 28º, $V_{\alpha C,\ Thr10,\ ads}$ = 0.7 Å^3).

The three homopolypeptides that do not accumulate to a measureable extent ($\sigma_{ads} < 0.5*10^3$ /μm^2) are Lys_{10}, Gln_{10} and Ala_{10}. Both lysine and glutamine have intermediate amino acid affinities for gold [$\Delta G_{ads,Lys}$ = -30.0 kJ/mol; $\Delta G_{ads,Gln}$ = -28.6 kJ/mol], but their unfavorable dynamic characteristics lead to little adsorption [$<C_{dhd}(2.5\ ns)>_{Lys10,\ ads.}$ = 10º, $V_{\alpha C,\ Lys10,\ ads}$ = 0.01 Å^3; $<C_{dhd}(2.5\ ns)>_{Gln10,\ ads.}$ = 8º, $V_{\alpha C,\ Gln10,\ ads}$ = 0.01 Å^3)]. This suggests that if either were incorporated in a peptide environment with decreased conformational stability, it would have significant binding. In our previous study of gold-binding peptides, we found that both peptide dynamics [$<C_{dhd}(2.5\ ns)>_{ads.}$ = 26 – 39º] and binding [56% of glutamine residues] were increased. For lysine, behavior depended on the peptide size. In the three repeat peptide, the peptide dynamics [$<C_{dhd}(2.5\ ns)>_{ads.}$ = 39º] and binding [66% of lysine residues bound] increase, whereas in the six repeat peptide, lysine binding is low [15%] despite high peptide dynamics [$<C_{dhd}(2.5\ ns)>_{ads.}$ = 26º]. We note that the dynamic characteristics of lysine in

solution are comparable to threonine, and are reduced more than the others on binding. Thus it is likely that the inability to change conformation after binding plays a large role in adsorption of this homopolypeptide. The exception to the correlation between experimentally observed homopolypeptide behavior and the combined influence of amino acid affinity and dynamic characteristics is Ala_{10}. This peptide resembles serine in that it has low amino acid affinity ($\Delta G_{ads,Ala}$ = -21.9 kJ/mol) and high flexibility ($<C_{dhd}(2.5\ ns)>_{Ala10,\ ads.}$ = 34º, $V_{\alpha C,\ Ala10,\ ads}$ = 2.0 Å^3. Unlike serine, the favorable dynamic behavior does not overcome the low affinity and lead to adsorption. As discussed above, it is likely that the favorable dynamic characteristics lead to self-aggregation in solution, limiting binding to gold. We conclude that the individual amino acids comprising a peptide interact with the surface to an extent determined by their chemical affinities. These affinities are realized to their full extent only when the peptide is flexible enough to enable conformational changes. Only then can the peptide explore many conformations at the surface, which both enables the search for conformations that maximize contact with the surface and lowers the entropic cost of adsorption. We have noticed above that flexibility and conformational change are related, and that both quantities follow similar trends regardless of whether the peptides are in solution or interacting with the gold surface.

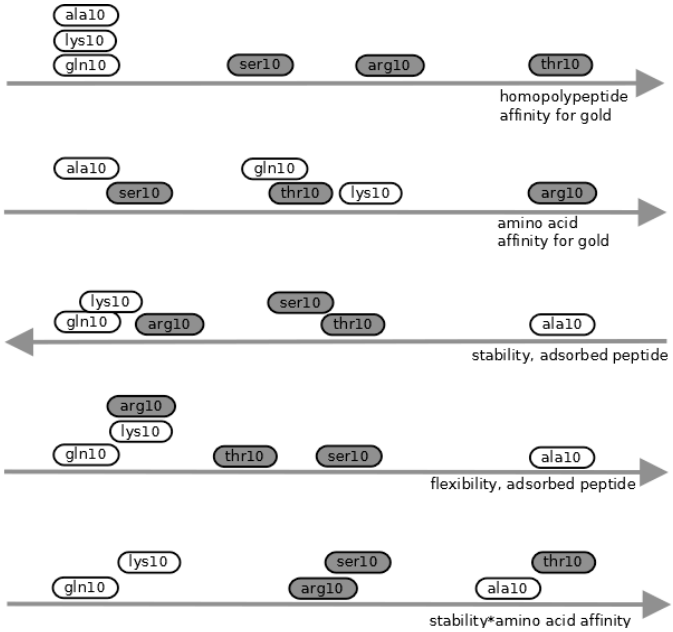

Figure 7. Schematic representation of the stability and flexibility of adsorbed homopolypeptides from our simulations. To facilitate comparisons, reported affinities of the same homopolypeptides and amino acids in solution are also shown.[12,15] The last line represents the product of the stability of adsorbed peptides from our simulations and reported affinities of amino acids in solution. Shaded boxes indicate homopolypeptides that adsorb to gold in experiments.

Concluding remarks: Determining new peptide sequences which bind to particular surfaces typically starts by designing peptide libraries for high-throughput combinatorial techniques. As binding depends both on peptide flexibility and enrichment in amino acids with high affinity for that surface, assessing both quantities is paramount. This knowledge can be used to design better peptide libraries to isolate new peptides with the desired binding characteristics. We investigated the role of conformational stability and flexibility on the affinity of the homopolypeptides Ser_{10}, Arg_{10}, Thr_{10}, Lys_{10}, Ala_{10} and Gln_{10} for gold surfaces using all-atom molecular dynamics simulations in explicit solvent. We have examined peptide conformational stability and flexibility before and after adsorption, and have found a positive correlation between low stability and experimentally determined higher affinity for gold. To explain this correlation we have investigated how the extent of adsorption during the early stages of peptide contact with gold depends on peptide conformational changes. We found that even rigid peptides may adsorb to some extent, but that extensive adsorption (where the percentage of adsorbed atoms > 50%) requires the peptide to change conformation for greater contact between the peptide and the surface. This observation explains the visible positive correlation between low peptide conformational stability (and high flexibility) and more extensive adsorption: peptides with lower conformational stability more easily explore multiple conformations at the surface and maximize the number of surface contacts. The present work is thus the first suggestion that observed homopolypeptide affinities for a surface reflect both the affinity of the amino acids for that surface and the intrinsic dynamical properties of the peptide. High affinity for gold surfaces arises only when the intrinsic surface affinity of the amino acids is high and the peptide remains conformationally flexible even after extensive contact with the gold surface. We note that the results outlined above are subject to the limitations of our approach: the short duration of the simulations compared with adsorption time-scales, the use of the fraction of adsorbed amino acids as a measure of the affinity of peptides for surfaces, and the use of a Lennard-Jones potential to model peptide-gold interactions, neglecting gold

polarization. Due to one or more of these limitations, the adsorption behavior in the simulations does not provide a quantitative measure of adsorption. The dynamic behavior of peptides, both in solution and following adsorption, is expected to be more accurate, although we do not have experimental results with which it may be directly compared. The most important contribution of this work relates these dynamics properties and individual amino acid affinities for gold[15] to experimental behavior.[12]

Acknowledgments

JKM acknowledges financial support from the US Department of Energy, Office of Advanced Scientific Computing; grant number DE-FG02-02ER25535. AVV acknowledges the Portuguese Foundation for Science and Technology for post-doctoral fellowship SFRH/BPD/20555/2004/0GVL. PJB acknowledges funding by the USA National Science Foundation Grant # EEC-0353569 for participation in the REU program in Biomolecular Engineering.

Supporting Information Available: The size of the simulated systems, details of the minimization and equilibration protocol followed, the original data for Figures 5 and 6, graphical representations of Arg_{10}'s conformational changes during adsorption and of the correlation between flexibility and stability can be found in the supporting information. This material is available free of charge via the Internet at http://pubs.acs.org.

Bibliography

(1) Ji, B. H.; Gao, H. J. *J. Mech. Phys. Solids* **2004**, *52*, (9), 1963-1990.

(2) Yao, N.; Epstein, A.; Akey, A. *J. Mat. Res.* **2006**, *21*, (8), 1939-1946.

(3) Kroger, N.; Deutzmann, R.; Sumper, M. *Science* **1999**, *286*, (5442), 1129-1132.

(4) Brown, S. *Nature Biotechnology* **1997**, *15*, (3), 269-272.

(5) Brown, S.; Sarikaya, M.; Johnson, E. *J. Mol. Biol.* **2000**, *299*, (3), 725-735.

(6) Naik, R. R.; Stringer, S. J.; Agarwal, G.; Jones, S. E.; Stone, M. O. *Nature Materials* **2002**, *1*, (3), 169-172.

(7) Kjargaard, K.; Sorensen, J. K.; Schembri, M. A.; Klemm, P. *Appl. Environ. Microbiol.* **2000**, *66*, (1), 10-14.

(8) Thai, C. K.; Dai, H.; Sastry, M. S. R.; Sarikaya, M.; Schwartz, D. T.; Baneyx, F. *Biotechnol. Bioeng.* **2004**, *87*, (2), 129-137.

(9) Whaley, S. R.; English, D. S.; Hu, E. L.; Barbara, P. F.; Belcher, A. M. *Nature* **2000**, *405*, (6787), 665-668.

(10) Naik, R. R.; Brott, L. L.; Clarson, S. J.; Stone, M. O. *J. Nanosci. Nanotechno.* **2002**, *2*, (1), 95-100.

(11) Kroger, N.; Deutzmann, R.; Bergsdorf, C.; Sumper, M. *Proc. Natl. Acad. Sci.USA* **2000**, *97*, (26), 14133-14138.

(12) Willett, R. L.; Baldwin, K. W.; West, K. W.; Pfeiffer, L. N. *Proc. Natl. Acad. Sci.USA* **2005**, *102*, (22), 7817-7822.

(13) In three letter code for amino acids.

(14) Iori, F.; Di Felice, R.; Molinari, E.; Corni, S. *J. Comput. Chem.* **2009**, *30*, (9), 1465-1476.

(15) Hoefling, M.; Iori, F.; Corni, S.; Gottschalk, K. E. *Langmuir* **2010**, *26*, (11), 8347-8351.

(16) Kokh, D. B.; Corni, S.; Winn, P. J.; Hoefling, M.; Gottschalk, K. E.; Wade, R. C. *J. Chem. Theory Comput.* **2010**, *6*, (5), 1753-1768.

(17) Liu, S. M.; Haynes, C. A. *J. Colloid Interf. Sci.* **2005**, *284*, (1), 7-13.

(18) Oren, E. E.; Notman, R.; Kim, W.; Evans, J. S.; Walsh, T. R.; Samudrala, R.; Tamerler, C.; Sarikaya, M. *Langmuir* **2010**, *26*, 11003-11009.

(19) Vila Verde, A.; Acres, J. M.; Maranas, J. K. *Biomacromolecules* **2009**, *10*, 2118-2128.

(20) Kacar, T.; Zin, M. T.; So, C.; Wilson, B.; Ma, H.; Gul-Karaguler, N.; Jen, A. K. Y.; Sarikaya, M.; Tamerler, C. *Biotechnol. Bioeng.* **2009**, *103*, (4), 696-705.

(21) Ibii, T.; Kaieda, M.; Hatakeyama, S.; Shiotsuka, H.; Watanabe, H.; Umetsu, M.; Kumagai, I.; Imamura, T. *Anal. Chem.* **2010**, *82*, (10), 4229-4235.

(22) Seker, U. O. S.; Wilson, B.; Sahin, D.; Tamerler, C.; Sarikaya, M. *Biomacromolecules* **2009**, *10*, (2), 250-257.

(23) So, C. R.; Tamerler, C.; Sarikaya, M. *Angew. Chem. Int. Edit.* **2009**, *48*, (28), 5174-5177.

(24) MacKerell, J. A. D.; Bashford, D.; Bellott, M.; Dunbrack Jr., R. L.; Evanseck, J. D.; Field, M. J.; Fischer, S.; Gao, J.; Guo, H.; Ha, S.; Joseph-McCarthy, D.; Kuchnir, L.; Kuczera, K.; Lau, F. T. K.; Mattos, C.; Michnick, S.; Ngo, T.; Nguyen, D. T.; Prodhom, B.; Reiher, I.; W.E.; Roux, B.; Schlenkrich, M.; Smith, J. C.; Stote, R.; Straub, J.; Watanabe, M.; Wiorkiewicz-Kuczera, J.; Yin, D.; Karplus, M. *J. Phys. Chem. B* **1998**, *102*, 3586-3616.

(25) Neria, E.; Fischer, S.; Karplus, M. *J. Chem. Phys.* **1996**, *105*, (5), 1902-1921.

(26) Calzolari, A.; Cicero, G.; Cavazzoni, C.; Di Felice, R.; Catellani, A.; Corni, S. *JACS* **2010**, *132*, (13), 4790-4795.

(27) Di Felice, R.; Selloni, A. *J. Chem. Phys.* **2004**, *120*, (10), 4906-4914.

(28) Kohlmeyer, A.; Witschel, W.; Spohr, E. *Chem. Phys.* **1996**, *213*, (1-3), 211-216.

(29) Berard, D. R.; Kinoshita, M.; Cann, N. M.; Patey, G. N. *J. Chem. Phys.* **1997**, *107*, (12), 4719-

4728.

(30) Shelley, J. C.; Berard, D. R. In *Reviews in computational Chemistry*, Lipkowitz, K. B.; Boyd, D. B., Eds. Wiley-VCH, John Wiley and Sons, Inc: 1998; Vol. 12, pp 137-205.

(31) Neves, R. S.; Motheo, A. J.; Fartaria, R. P. S.; Fernandes, F. M. S. S. *J. Electroanal. Chem.* **2007**, *609*, (2), 140-146.

(32) Phillips, J. C.; Braun, R.; Wang, W.; Gumbart, J.; Tajkhorshid, E.; Villa, E.; Chipot, C.; Skeel, R. D.; Kale, L.; Schulten, K. *J. Comput. Chem.* **2005**, *26*, (16), 1781-1802.

(33) Humphrey, W.; Dalke, A.; Schulten, K. *J. Mol. Graphics.* **1996**, *14*, (1), 33-38.

(34) Chivian, D.; Kim, D. E.; Malmstrom, L.; Schonbrun, J.; Rohl, C. A.; Baker, D. *Proteins Struct. Funct. Bioinf.* **2005**, *61*, 157-166.

(35) Altschuler, E. L.; Hud, N. V.; Mazrimas, J. A.; Rupp, B. *Febs Letters* **2000**, *472*, (1), 166-167.

(36) Pace, C. N.; Scholtz, J. M. *Biophys. J.* **1998**, *75*, (1), 422-427.

(37) Wang, X.; Vitalis, A.; Wyczalkowski, M.; Pappu, R. *Proteins Struct. Funct. Bioinf.* **2006**, *63*, (2), 297-311.

(38) Caesar, C. E. B.; Esbjorner, E. K.; Lincoln, P.; Norden, B. *Biochemistry* **2006**, *45*, (24), 7682-7692.

(39) Doruker, P.; Bahar, I. *Biophys. J.* **1997**, *72*, (6), 2445-2456.

(40) Xiong, K.; Asciutto, E. K.; Madura, J. D.; Asher, S. A. *Biochemistry* **2009**, *48*, (45), 10818-10826.

(41) Schaftenaar, G.; Noordik, J. H. *J. Comput. Aid. Mol. Des.* **2000**, *14*, (2), 123-134.

(42) Schroder, C.; Rudas, T.; Boresch, S.; Steinhauser, O. *J. Chem. Phys.* **2006**, *124*, (23).

(43) Prestrelski, S. J.; Williams, A. L.; Liebman, M. N. *Abstr. Pap. Am. Chem. S.* **1989**, *197*, 2-COMP.

(44) Heinz, H.; Farmer, B. L.; Pandey, R. B.; Slocik, J. M.; Patnaik, S. S.; Pachter, R.; Naik, R. R.

JACS **2009**, *131*, (28), 9704-9714.

(45) Braun, R.; Sarikaya, M.; Schulten, K. *J. Biomater. Sci. Polymer Edn* **2002**, *13*, 747 – 757.

(46) Giri, K.; Bhattacharyya, N. P.; Basak, S. *Biophys. J.* **2007**, *92*, (1), 293-302.

(47) In our previous work we also examined a peptide 42 amino acids long, i.e. with intermediate length.[19] We found that its stability actually decreased upon adsorption suggesting that the effect of adsorption on peptide stability may differ substantially, depending on the structure, structural stability and flexibility of the free peptide. Here we restrict our conclusions to peptides whose stability increases upon adsorption.

Table of contents only